Optimization of aircraft wake alleviation schemes through an Evolution Strategy

Philippe Chatelain*, Mattia Gazzola, Stefan Kern**, and Petros Koumoutsakos

Chair of Computational Science
ETH Zurich, CH-8092 Zurich, Switzerland
philippe.chatelain@uclouvain.be,mattia.gazzola@inf.ethz.ch,
kerns@ge.com,petros@inf.ethz.ch
http://www.cse-lab.ethz.ch

Abstract. We investigate schemes to accelerate the decay of aircraft trailing vortices. These structures are susceptible to several instabilities that lead to their eventual destruction. We employ an Evolution Strategy to design a lift distribution and a lift perturbation scheme that minimize the wake hazard as proposed in [6]. The performance of a scheme is measured as the reduction of the mean rolling moment that would be induced on a following aircraft; it is computed by means of a Direct Numerical Simulation using a parallel vortex particle code. We find a configuration and a perturbation scheme characterized by an intermediate wavelength $\lambda \sim 4.64$, necessary to trigger medium wavelength instabilities between tail and flap vortices and subsequently amplify long wavelength modes.

Keywords: Large Scale Simulations in CS&E, Parallel and Distributed Computing, Numerical Algorithms for CS&E

1 Introduction

Aircraft trailing vortices are powerful flow structures inherent to the very production of lift along the wing. These structures live long after an aircraft has flown by and constitute a potential hazard to any following aircraft. As a consequence, they require the enforcement of strict separation distances in particular at take-off and landing. This phenomenon is the limiting constraint on airport traffic, not without environmental consequences: longer traffic patterns lead to more noise and air pollution in particular.

The design of schemes to accelerate the decay of trailing vortices have been the topics of several theoretical [7, 5], experimental [6] and numerical investigations [1, 16].

* Present address: Institute of Mechanics, Materials and Civil Engineering, Université catholique de Louvain, B-1348 Louvain-la-Neuve, Belgium

** Present address: GE Global Research - Europe, D-85748 Garching bei München, Germany

The design and optimization of a wake alleviation scheme is a complex engineering problem. Wake decay simulations require solving the full three-dimensional Navier-Stokes well into the non-linear regime of vortex instabilities. These results then allow the measurement of the hazard level. This is a highly non-linear and multi-modal optimization problem, which does not lend itself to gradient-based methods.

In this work, we couple a derandomized Evolution Strategy with Covariance-Matrix Adaptation (CMA-ES) to a fast parallel Navier-Stokes solver in order to design and optimize a wake alleviation scheme. We base our work on an approach proposed in [6]. We note that integrated optimization approaches have been used before, albeit at a smaller scale [14].

This paper is organized as follows. Section 2 presents the problem of wake alleviation and its statement as an optimization problem. Section 3 presents the optimization and numerical tools of our study. In Section 4, we present our results.

2 Optimization of wake alleviation

2.1 Alleviation scheme

We investigate the scheme proposed in [6]. This scheme relies on the periodic deflection of wing control surfaces (flaps) in order to perturb the near wake of the aircraft where there are several pairs of trailing vortices. The periodic control surface motions redistribute some lift between the inboard and outboard sections of the wing. This redistribution conserves the total lift –although not necessarily the pitching moment of the wing–, the circulation, and a zero rolling moment. The effect is a periodic oscillation of the positions of the tip and inboard flap vortices. This forced an accelerated reconnection of the tip vortices, at a rate which can be about twice as high as the regular Crow instability[6].

We will use the same perturbation amplitude as in [6] and redistribute $\Delta C_L/C_L = 6\%$ of the total wing lift.

2.2 Optimization of the lift distribution and perturbation

In this section we describe the cost function, the parameterization of the problem and the search space.

Cost function In the context of our optimization procedure,we will approximate the hazard posed to a following aircraft (with a wing span b_{follow}) by the maximum rolling moment averaged in the streamwise direction. We define the induced rolling moment as

$$C_{\text{roll}}(x, y, z, t) = \int_{y-1/2b_{\text{follow}}}^{y+1/2b_{\text{follow}}} (y' - y) u_z(x, y, z, t) dy' \tag{1}$$

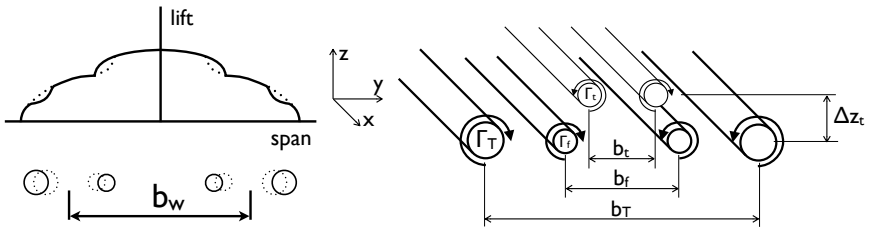

(a) Lift redistribution and effect on vortices

(b) Unperturbed trailing vortices

Fig. 1: Wing and wake configuration

and its streamwise average as

$$\langle C_{\text{roll}} \rangle_x (y, z, t) = \frac{1}{L_x} \int_0^{L_x} C_{\text{roll}}(x, y, z, t) dx \ . \tag{2}$$

We opt to define our cost function as the maximum average rolling moment

$$f_{\text{obj}} = \max_{y,z \in [-\infty, +\infty]} \langle C_{\text{roll}} \rangle_x (y, z, \tau_{\text{obj}}) \tag{3}$$

taken at a fixed dimensionless time $\tau_{\text{obj}} = 5$ and for a $b_{\text{follow}} = 1/2 b_w$. This descent time value corresponds to a downstream distance of $\sim 4nm$, which matches the ICAO Standard Separation Distance between large jumbo jets. This mandatory separation grows to $6nm$ if the following aircraft is a light aircraft, justifying wake destruction within this time and space interval.

Parameterization and search space We study the time evolution of the trailing vortices under the approximation of a streamwise periodic flow. The wake configuration is sketched in Fig. 1b. We account for the wing lift distribution through the geometry of the flap and tip vortices; they have, respectively, the circulations Γ_f and Γ_T and the spans b_f and b_T. The wing circulation and equivalent span can then be written as

$$\Gamma_w = \Gamma_T + \Gamma_f \tag{4}$$

$$b_w = \frac{\Gamma_T}{\Gamma_w} b_T + \frac{\Gamma_f}{\Gamma_w} b_f \tag{5}$$

The negative lift of the horizontal tail plane (HTP) is manifested by a third vortex pair with circulation Γ_t and span b_t. Because this pair is generated downstream of the wing, we assume it to be positioned Δz_t above the wing and flap vortices. These vortices are assumed to be Gaussian with core sizes σ_T, σ_f and σ_t.

The dimensionality of our search space will be sensibly smaller than the number of parameters outlined above as we choose to constrain several engineering characteristics of the problem. The total wing lift, proportional to $\Gamma_w b_w$, and the root wing circulation Γ_w have to be preserved. The lift redistribution is kept at $\Delta C_L/C_L = 6\%$ of the total wing lift. The HTP keeps the same negative lift and the vortex core sizes do not change. The resulting search space then counts 4 parameters

$\alpha = 2\pi/\lambda$ is the wavenumber of the perturbation;
$\beta = b_t/b_w$ is the span of the HTP vortices;
$\gamma = \Gamma_f/\Gamma_w$ is the circulation ratio of the flap vortices;
$\delta = (b_T - b_f)/(2b_w)$ is the separation between the tip and flap vortices.

The remaining parameters are kept constant and listed in the Table 1a. We bound the configuration parameters in order to avoid unfeasible or physically irrelevant configurations. The bounds are summarized in Table 1b.

Parameter	Value
Γ_w/ν	2500
$\Gamma_t b_t$	$-0.0836\,\Gamma_w b_w$
σ_T	$0.05\,b_w$
σ_f	$0.05\,b_w$
σ_t	$0.025\,b_w$

(a) Constants

Parameter	Minimun	Maximum
α	0.5	5.0
β	0.2	0.5
γ	0.1	0.5
δ	0.25	0.5

(b) Ranges

Table 1: Parameters

3 Methodology

3.1 Vortex particle method

We consider a three dimensional incompressible flow and the Navier-Stokes equations in its velocity ($\mathbf{u}$)-vorticity ($\boldsymbol{\omega} = \nabla \times \mathbf{u}$) form :

$$\frac{D\boldsymbol{\omega}}{Dt} = (\boldsymbol{\omega} \cdot \nabla)\,\mathbf{u} + \nu \nabla^2 \boldsymbol{\omega} \tag{6}$$

$$\nabla \cdot \mathbf{u} = 0 \tag{7}$$

where $\frac{D}{Dt} = \frac{\partial}{\partial t} + \mathbf{u} \cdot \nabla$ denotes the Lagrangian derivative and ν is the kinematic viscosity. Vortex methods discretize the vorticity field with particles, characterized by a position $\mathbf{x}_p$, a volume V_p and a strength $\boldsymbol{\alpha}_p = \int_{V_p} \boldsymbol{\omega} d\mathbf{x}$. Particles are convected by the flow field and their strength is modified to account for vortex stretching and diffusion.

Using the definition of vorticity and the incompressibility constraint the velocity field is computed by solving the Poisson equation

$$\nabla^2 \mathbf{u} = -\nabla \times \boldsymbol{\omega} \; . \tag{8}$$

This equation will be solved on a grid by means of a Fourier solver that allows for mixed periodic (x) and unbounded directions (y and z). We use remeshing[3, 10, 15] in order to remedy the loss of accuracy due to Lagrangian distortion. Remeshing consists in the periodic regularization onto a grid of the particle set via high order interpolation In the present work, remeshing is performed at the end of each time step and uses the third order accurate M_4' interpolation formula of [11]. The grid/mesh allows for additional advances: differential operators (such as those for stretching and diffusion) are evaluated on the mesh using fourth order finite differences and the Poisson equation (Eq. 8) is solved on the grid. The results of these calculations on the grid are then interpolated back onto the particles. We refer to [1, 2] for details on the parallel implementation and the periodic-unbounded Poisson solver.

The vortex particle method is particularly well-suited for our flow configuration. It exploits the compact support of vorticity: particles are only needed where vorticity is non-zero. Likewise, the grid of the unbounded-periodic Poisson solver tracks the support of vorticity and grows or shrinks accordingly in the transverse directions. Finally, the method exhibits accuracy, robustness and relaxed stability properties for advection[4].

3.2 Evolution Strategy

We use a state-of-the-art Evolution Strategy with Covariance Matrix Adaptation (CMA-ES)[8]. CMA-ES belongs to the class of Evolutionary Algorithms comprising methods that are inspired by the principles of natural evolution to solve optimization and learning problems. It is operating with real valued parameters and adapts a Gaussian sampling distribution from the information acquired in the course of the optimization.

The gradient of the cost function in the search space is not readily available in the present investigation: an adjoint approach would be impractical and Finite Differences involve a stepsize selection procedure. The need for robustness and the likelihood of local minima in the cost function therefore close the case for CMA-ES. This requirement of robustness and the dimensionality of the problem (4) impose the population size of the Evolution Strategy, i.e. the number of function evaluations needed at every iteration of CMA-ES. We set it to 10 based on the investigations in [9].

Finally, we note that the search space is bounded through the constraints of Table 1b. These boundaries are enforced by biasing the sampling distributions, i.e. through a rejection algorithm.

3.3 Coupling and computation

Every evaluation of the cost function is carried out by our parallel vortex particle code[1] and can involve running on hundreds of processors for several hours. Our

approach consisted in dissociating this evaluation process from the optimization code. The latter is not computationally intensive and can easily run on a personal workstation; the former requires access to parallel architectures counting several hundred cores, typically in a supercomputing center, enabling the fast evaluation of several candidates of a population in parallel. This allows us to use an existing CMA-ES matlab implementation[1] and to only implement the evaluation of the cost function.

This matlab function determines the computational problem size from well-resolvedness considerations and then chooses a supercomputer partition size that keeps the wallclock duration of a simulation approximately constant (here between 4 and 12 hours). It generates the control files and scripts necessary to submit the parallel job on the super-computer queue, copies them and submits the job remotely. Several jobs –10 in this study– are submitted at the same time as they correspond to the function evaluations inside an iteration of CMA-ES. Their statuses are monitored and upon completion, their results are copied back in order to post-process them and return a scalar $f_{\mathrm{obj}}(\mathbf{x})$.

4 Results

4.1 Optimization

The history of the optimization is shown in Fig. 2. We see that CMA-ES went through 34 iterations, or 340 evaluations. The evaluations resulted in simulations running on Cray XT5 partitions ranging from 64 to 256 cores for run times between 6 and 12 wallclock hours. This represents a total of $270,000$ CPU hours.

The optimization was initialized in the center of our parameter intervals and converged (see Fig. 2) to a point which reduces the wake hazard by a factor of 4 with respect to the initial guess.

4.2 Optimum parameter set

The best candidate found over the course of the optimization is the case 174; it is described by the parameters $(\alpha, \beta, \gamma, \delta) = (1.3544, 0.48186, 0.47542, 0.48261)$. After encountering this point, the Evolution Strategy searches its neighborhood and eventually converges to this point (see Fig. 2b).

This candidate is characterized by a wavelength $\lambda = 4.64\, b_w$ sensibly smaller than the wavelength of the Crow instability for the equivalent wing vortex pair $\lambda_{\mathrm{Crow}} \sim 8\, b_w$. Fig. 3 shows the evolution of the flow. The early phase is characterized by the fast growth of medium wavelength instabilities between the tail and flap vortices (see Fig. 3b and Fig. 3c). The reconnections generate dipoles similar to Ω-loops[12] which perturb the tip vortices and reconnect with them (Fig. 3d).

The outstanding features of the optimum become more apparent in a comparison with another less performant candidate. Fig. 4 shows the development

[1] available at www.cse-lab.ethz.ch

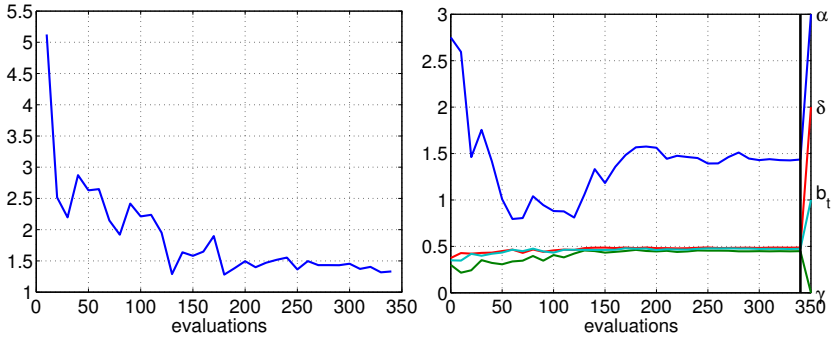

(a) f_{obj} (b) Parameters

Fig. 2: CMA-ES optimization history: evolution of the best cost function achieved in current generation and parameters.

of the best candidate of the first iteration (case 2), described by $(\alpha, \beta, \gamma, \delta) = (2.1606, 0.37654, 0.13392, 0.42296)$ and thus a wavelength $\lambda = 2.91$. This case shows that even though its vortex dynamics produce a fast growing medium-wavelength instability between the flap and tail vortices, they do not perturb the tip vortices appreciably. The flow generates large dipoles (Fig. 4b and 4c) which get twirled around the tip vortices (Fig. 4d). This leads to fairly large secondary structures (Fig. 4e) but keeps the tip vortices relatively straight and unaffected.

In the optimum case, the transverse structures are smaller but more importantly, the tip vortices are displaced vertically over a half wavelength (Fig. 3c to 3f). In fact, this segmentation of the tip vortices is even apparent in the contours of the average rolling moment, shown in Fig. 5. The cores are distinguishable at two levels (Fig. 5d) thus causing the average moment to be roughly halved along the axes of these cores.

This effect appears to contribute substantially to the overall dissipation of the wake. And even more so if we consider the rolling moments of case 2 where there is no vertical spreading of the cores or halving of the average moment(Fig. 6).

5 Conclusions

We have coupled a derandomized Evolution Strategy and an efficient parallel Navier-Stokes solver in order to optimize a wake alleviation scheme. The optimization relied on the parameterization of the wake configuration and the use of a wake hazard measurement for the cost function. Convergence of the ES required hundreds of function evaluations which were computed remotely on a supercomputing cluster.

An optimum was found at an intermediate wavelength $\lambda = 4.64 b_w$. For typical approach speeds, this corresponds to an actuation frequency which is in

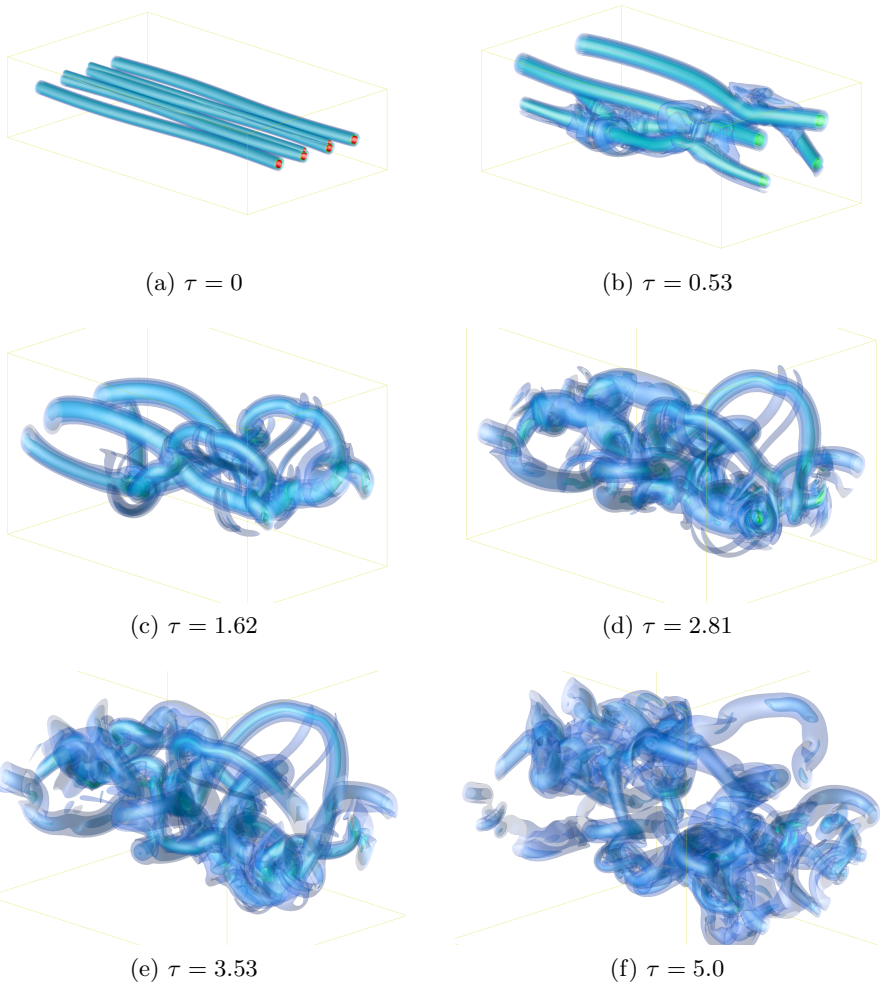

(a) $\tau = 0$ (b) $\tau = 0.53$

(c) $\tau = 1.62$ (d) $\tau = 2.81$

(e) $\tau = 3.53$ (f) $\tau = 5.0$

Fig. 3: Optimum parameter set (case 174): isosurfaces of vorticity norm $\|\boldsymbol{\omega}\| = 0.01,\ 0.02,\ 0.04,\ 0.08\, \Gamma_w/(\pi\sigma_T^2)$

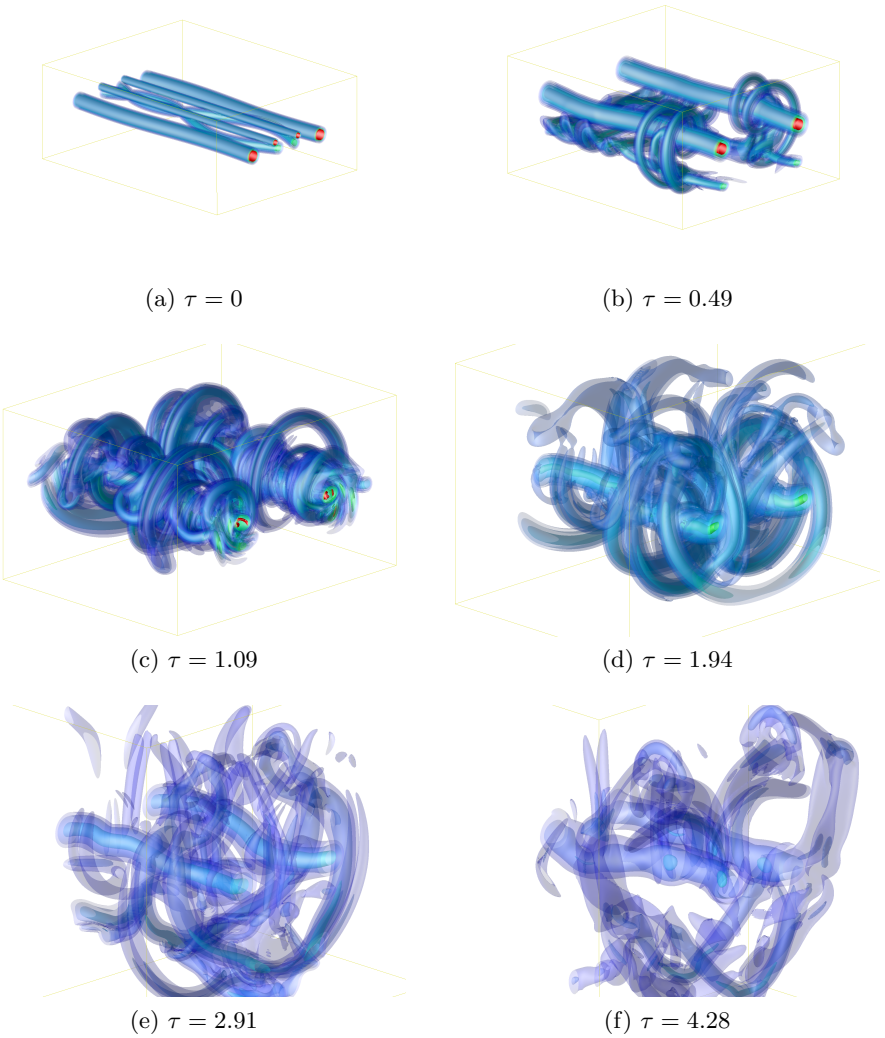

(a) $\tau = 0$ (b) $\tau = 0.49$

(c) $\tau = 1.09$ (d) $\tau = 1.94$

(e) $\tau = 2.91$ (f) $\tau = 4.28$

Fig. 4: Best candidate of the first generation (case 2): isosurfaces of vorticity norm $\|\boldsymbol{\omega}\| = 0.01,\ 0.02,\ 0.04,\ 0.08\, \Gamma_w/(\pi\sigma_T^2)$

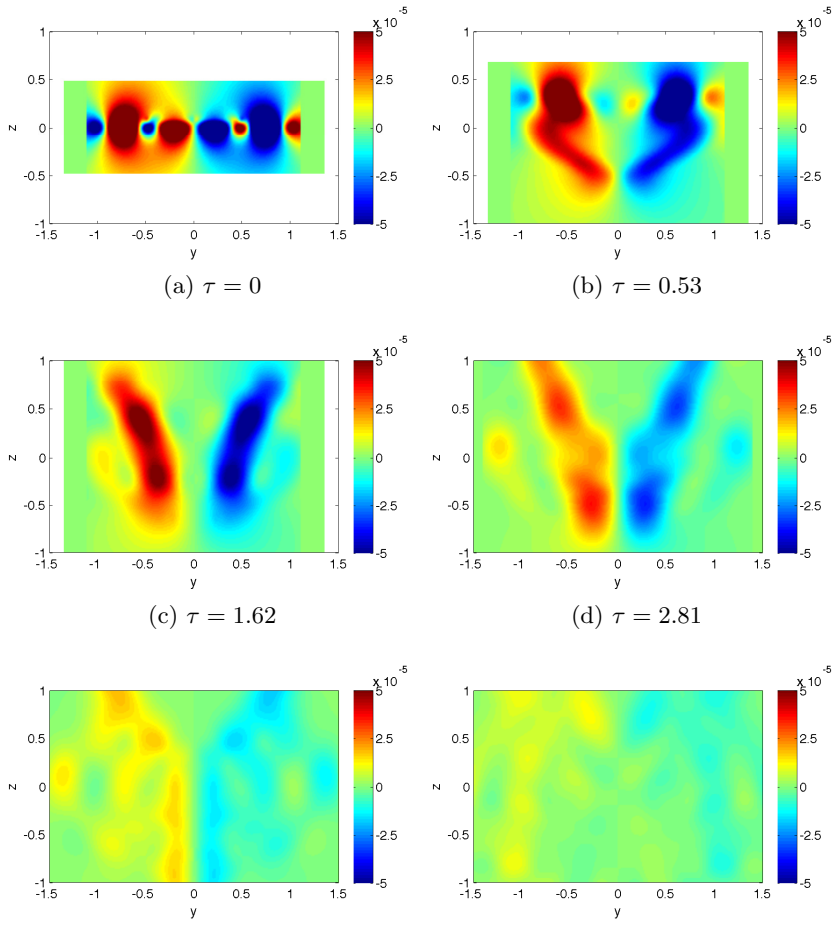

(a) $\tau = 0$ (b) $\tau = 0.53$

(c) $\tau = 1.62$ (d) $\tau = 2.81$

(e) $\tau = 3.53$ (f) $\tau = 5.0$

Fig. 5: Optimum parameter set (case 174): streamwise-averaged rolling moment $\langle C_{\mathrm{roll}} \rangle_x$

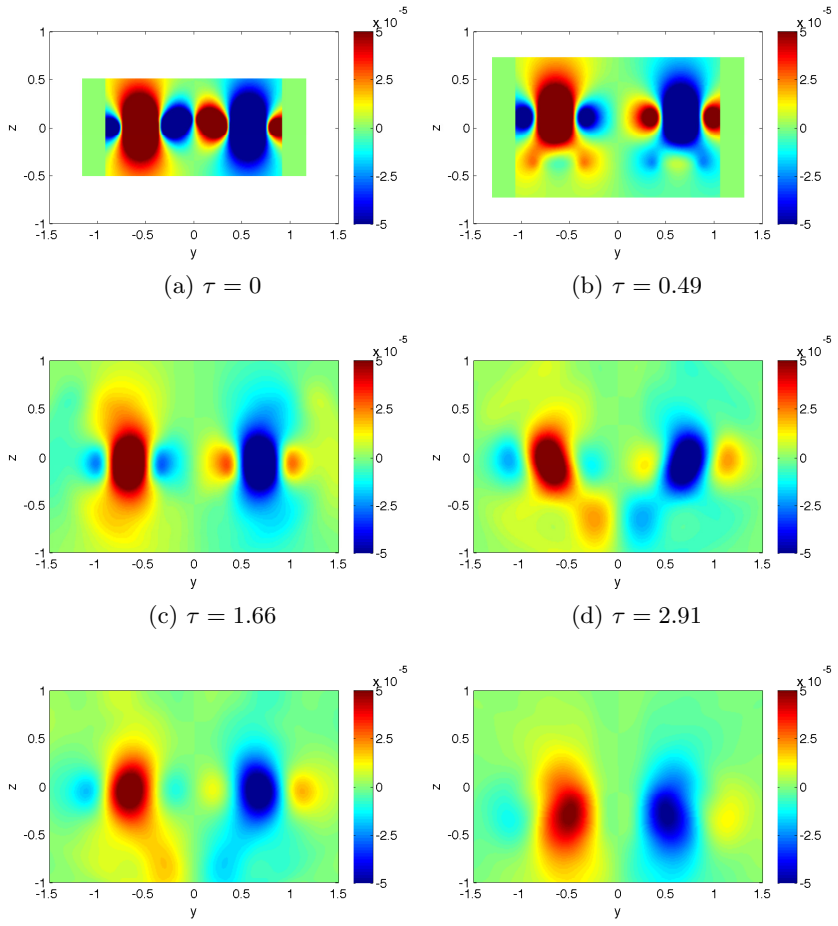

(a) $\tau = 0$ (b) $\tau = 0.49$

(c) $\tau = 1.66$ (d) $\tau = 2.91$

(e) $\tau = 3.56$ (f) $\tau = 5.0$

Fig. 6: Best candidate of the first generation (case 2): streamwise-averaged rolling moment $\langle C_{\text{roll}} \rangle_x$

the sub-Hertz range $f \sim 0.2 - 0.4$Hz. The perturbation triggers fast-growing medium wavelength instabilities and vortex reconnections. The resulting flow disrupts the tip vortices and smears their induced rolling moment.

The present results were obtained from Direct Numerical Simulations at a moderate Reynolds number of 2500. While it may be argued that this mimics a uniform turbulent viscosity (see [13]), this constitutes a very crude RANS and future simulations will be carried out with an actual LES model.

Other future work areas include the addition of noise in the initial conditions in order to favor robust alleviation schemes over the course of the optimization. In addition, the cost function based on a fixed time measurement will be abandoned in favor of a time window average of the wake hazard. Finally, we plan to account for the spatial development of the flow and track the actuation effects more realistically. We will simulate the perturbed lift distribution itself, capture its effect in the near wake and then start a streamwise periodic simulation from the established vortex wake field.

Acknowledgments

The computational resources were provided by the Swiss Supercomputing Center (CSCS).

References

1. P. Chatelain, A. Curioni, M. Bergdorf, D. Rossinelli, W. Andreoni, and P. Koumoutsakos. Billion vortex particle direct numerical simulations of aircraft wakes. *Computer Methods in Applied Mechanics and Engineering*, 197(13):1296–1304, Feb 2008.
2. P. Chatelain and P. Koumoutsakos. A fourier-based elliptic solver for vortical flows with periodic and unbounded directions. *Journal of Computational Physics*, 229(7):2425–2431, 4 2010.
3. G.-H. Cottet. Artificial viscosity models for vortex and particle methods. *J. Comput. Phys.*, 127(2):299–308, 1996.
4. G.-H. Cottet and P. Koumoutsakos. *Vortex Methods, Theory and Practice*. Cambridge University Press, 2000.
5. J. D. Crouch. Instability and transient growth for two trailing-vortex pairs. *Journal of Fluid Mechanics*, 350:311–330, 1997.
6. J. D. Crouch, G. D. Miller, and P. R. Spalart. Active-control system for breakup of airplane trailing vortices. *AIAA Journal*, 39(12):2374–2381, Dec 2001.
7. S. C. Crow. Stability theory for a pair of trailing vortices. *AIAA Journal*, 8(12):2172–2179, 1970.
8. N. Hansen, S. D. Muller, and P. Koumoutsakos. Reducing the time complexity of the derandomized evolution strategy with covariance matrix adaptation (cma-es). *Evolutionary Computation*, 11(1):1–18, Spr 2003.
9. S. Kern. *Bioinspired optimization algorithms for the design of anguilliform swimmers*. PhD thesis, ETH Zurich, 2007.
10. P. Koumoutsakos. Inviscid axisymmetrization of an elliptical vortex. *J. Comput. Phys.*, 138(2):821–857, 1997.

11. J. J. Monaghan. Extrapolating b splines for interpolation;. *Journal of Computational Physics*, 60(2):253–262, 1985.
12. J. M. Ortega, R. L. Bristol, and Ö. Savas. Experimental study of the instability of unequal-strength counter-rotating vortex pairs. *Journal of Fluid Mechanics*, 474:35–84, Jan 2003.
13. P.R Owen. The decay of a turbulent trailing vortex. *Aeronautical Quarterly*, 21:69–78, 1970.
14. E. Stumpf. Study of four-vortex aircraft wakes and layout of corresponding aircraft configurations. *J. Aircraft*, 42(3):722–730, 2005.
15. G. Winckelmans. Vortex methods. In Erwin Stein, René De Borst, and Thomas J.R. Hughes, editors, *Encyclopedia of Computational Mechanics*, volume 3. John Wiley and Sons, 2004.
16. G. Winckelmans, R. Cocle, L. Dufresne, and R. Capart. Vortex methods and their application to trailing wake vortex simulations. *C. R. Phys.*, 6(4-5):467–486, 2005.